AD-A060 797 MISSION RESEARCH CORP SANTA BARBARA CALIF F/G 18/3
INCLUSION OF EARTH REFLECTED FIELDS IN THE HIGH ALTITUDE EMP CO--ETC(U)
MAY 78 W E HOBBS DNA001-77-C-0135
UNCLASSIFIED MRC-R-377 DNA-4536T NL

| OF |
AD
A060797

END
DATE
FILMED
01 -79
DDC

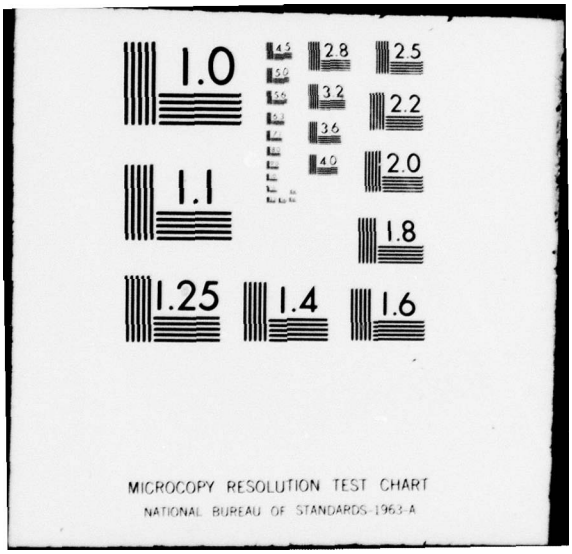
1.0
1.1
1.25
1.4
1.6
1.8
2.0
2.2
2.5
2.8
3.2
3.6
4.0
MICROCOPY RESOLUTION TEST CHART
NATIONAL BUREAU OF STANDARDS-1963-A

AD-E300 348

(12) LEVEL II

DNA 4536T

AD A060797

DDC FILE COPY

INCLUSION OF EARTH REFLECTED FIELDS IN THE HIGH ALTITUDE EMP CODE LHAP

Mission Research Corporation
735 State Street
Santa Barbara, California 93101

May 1978

Topical Report for Period 3 January 1977—31 March 1978

CONTRACT No. DNA 001-77-C-0135

APPROVED FOR PUBLIC RELEASE;
DISTRIBUTION UNLIMITED.

THIS WORK SPONSORED BY THE DEFENSE NUCLEAR AGENCY
UNDER RDT&E RMSS CODE B323077464 R99QAXEA09172 H2590D.

Prepared for
Director
DEFENSE NUCLEAR AGENCY
Washington, D. C. 20305

DDC
RECEIVED
NOV 6 1978
B

78 09 28 080

Destroy this report when it is no longer needed. Do not return to sender.

PLEASE NOTIFY THE DEFENSE NUCLEAR AGENCY, ATTN: TISI, WASHINGTON, D.C. 20305, IF YOUR ADDRESS IS INCORRECT, IF YOU WISH TO BE DELETED FROM THE DISTRIBUTION LIST, OR IF THE ADDRESSEE IS NO LONGER EMPLOYED BY YOUR ORGANIZATION.

UNCLASSIFIED

SECURITY CLASSIFICATION OF THIS PAGE (When Data Entered)

REPORT DOCUMENTATION PAGE

READ INSTRUCTIONS BEFORE COMPLETING FORM

1. REPORT NUMBER: DNA 4536T

2. GOVT ACCESSION NO.:

3. RECIPIENT'S CATALOG NUMBER:

4. TITLE (and Subtitle): INCLUSION OF EARTH REFLECTED FIELDS IN THE HIGH ALTITUDE EMP CODE LHAP.

5. TYPE OF REPORT & PERIOD COVERED: Topical Report for Period 3 Jan 77—31 Mar 78

6. PERFORMING ORG. REPORT NUMBER: MRC-R-377

7. AUTHOR(s): W. E. Hobbs

8. CONTRACT OR GRANT NUMBER(s): DNA 001-77-C-0135

9. PERFORMING ORGANIZATION NAME AND ADDRESS:
Mission Research Corporation
735 State Street
Santa Barbara, California 93101

10. PROGRAM ELEMENT, PROJECT, TASK AREA & WORK UNIT NUMBERS: NWED Subtask R99QAXEA091-72

11. CONTROLLING OFFICE NAME AND ADDRESS:
Director
Defense Nuclear Agency
Washington, D.C. 20305

12. REPORT DATE: May 1978

13. NUMBER OF PAGES: 30

14. MONITORING AGENCY NAME & ADDRESS (if different from Controlling Office): 29 p.

15. SECURITY CLASS (of this report): UNCLASSIFIED

15a. DECLASSIFICATION/DOWNGRADING SCHEDULE:

16. DISTRIBUTION STATEMENT (of this Report)

Approved for public release; distribution unlimited.

DNA, SBIE / 4536T, AD-E300 348

17. DISTRIBUTION STATEMENT (of the abstract entered in Block 20, if different from Report)

18. SUPPLEMENTARY NOTES

This work sponsored by the Defense Nuclear Agency under RDT&E RMSS Code B323077464 R99QAXEA09172 H2590D.

19. KEY WORDS (Continue on reverse side if necessary and identify by block number)

Electromagnetic Pulse (EMP)
Nuclear Weapons Effects
High Altitude EMP
Ground Effects
Reflected Pulse
Conducting Dielectric

20. ABSTRACT (Continue on reverse side if necessary and identify by block number)

Fields reflected from the ground affect calculations of the high-altitude-burst EMP at times later than about 100 microseconds. A simple procedure has been developed for calculating the reflected fields and the LHAP code has been modified to include these fields in the calculation of the total EMP. With this modification the LHAP calculations are valid up to about one millisecond.

DD FORM 1 JAN 73 1473 EDITION OF 1 NOV 65 IS OBSOLETE

UNCLASSIFIED

SECURITY CLASSIFICATION OF THIS PAGE (When Data Entered)

406 548 78 09 28 080 LB

PREFACE

The author would like to thank H. J. Longley and C. L. Longmire for many illuminating discussions during the course of this research. J. Gilbert had the great insight to point out the method of solving the reflected wave using a convolution integral and H. Price explained that only the real part of the reflection coefficient is needed in establishing the response function. C. L. Longmire pointed out the straightforward method for fitting the response function and was very helpful with the manuscript.

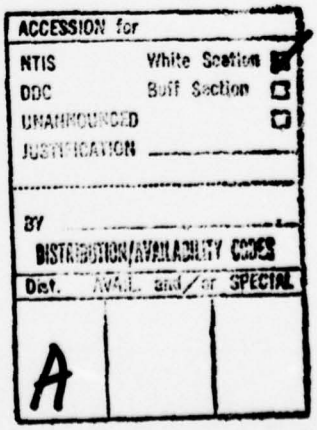

CONTENTS

ILLUSTRATIONS

SECTION 1
INTRODUCTION

The EMP from high altitude nuclear explosions is traditionally calculated in several time phases. In the earliest time phase, which covers times from zero to about one microsecond, only time and radial derivatives in Maxwell's equations are significant, and only the Compton current produced by previously unscattered gamma rays is important. In this time phase the self-consistent codes CHAP and HEMP-B give quite accurate calculations of the EMP. In the time phase from one microsecond to about one millisecond, scattered gammas become an important source and the transverse derivatives in the vertical plane (of the ray from burst to observer) are not negligible, whereas azimuthal derivatives are still not important. In this case, Maxwell's equations can be reduced to a set of equations in one time variable (the retarded time) and one space variable (essentially the vertical coordinate), in the approximation that the gamma-ray front is planar (i.e., the burst is assumed to be far away), and the curvature of the earth is neglected. This constitutes the far-plane approximation[1] upon which the code LHAP[2] is based. The EMP fields in this time phase are not large enough to require self-consistent treatment of the Compton recoil electrons, and an approximate but fairly accurate treatment of the Compton current was devised to increase the speed of the computations.

Previously, the LHAP code has been run only up to retarded times of 100 microseconds. This is approximately the time when the EMP reflected from the surface of the earth re-enters the source region, and the code had no capability for handling the reflected pulse. In the present report we devise a method for including the reflected fields in LHAP so that it can be

[illegible]

run to later times. The aim is to compute up to about one millisecond, after which other LHAP approximations break down.

The reflection of EM waves from the earth's surface is an old problem, and is solved well in the Fourier domain by the Fresnel reflection factors.[3] Several codes and approximate methods[4,5] have been constructed to calculate the reflected EMP. Most of these methods Fourier transform the EMP time wave form, apply the Fresnel reflection factor, and Fourier invert to find the time wave form of the reflected pulse. For the LHAP problem this is not a convenient method for two reasons. First, the reflected fields are needed at times when the calculation of the incident fields is still in process; thus one would have to break the total incident pulse into pieces of length equal to the delay time from source region to ground and back, and reflect each piece. Second, the processes of Fourier transforming and inverting are time consuming. It is better to transform the Fresnel reflection factor to the time domain in the beginning, for example, by obtaining the reflected fields for an impulse incident pulse. This gives a kernel $G(t-t')$, and the convolution of this kernel with an arbitrary incident pulse $E_i(t)$ gives the reflected pulse $E_r(t)$,

$$E_r(t) = \int_{t'=-\infty}^{t} G(t-t')E_i(t')dt' \quad .$$

This method requires doing the convolution integral at each time step. Now, if the kernel is approximated as a finite sum of N decaying exponentials, the convolution integral can be replaced by a set of N first order differential equations. The solution of these equations needs only to be advanced one time step per LHAP time step, and the computing time required is minuscule.

This is the method that we shall use. It is equivalent to approximating the Fresnel reflection factor in the Fourier domain as a sum of poles $1/(\omega+ib_n)$.

SECTION 2
LHAP GEOMETRY

The physical situation is shown in Figure 1. The plasma gamma-ray front is shown at two points in time $(t_2 > t_1)$. The ground plane and the dashed planes limiting the desposition region are also shown. Each star depicted is at the same point in space relative to the nearer gamma-ray front. We assume that the sources at star (1) and time t_1, are the same as those at star (2) and time t_2. The fields therefore must be functions only of the time after the initial gamma-ray front passed and the altitude. In the code LHAP[2] the independent variables are defined as

$$\begin{aligned} \tau &= ct - y = \text{retarded time in length units} \\ \eta &= z - (\tan\theta)y = \text{slant height above ground} \end{aligned} \tag{1}$$

where y is the space coordinate in the direction $\vec{n}$ of propagation of the gamma-ray front, z is the coordinate directed up the wave front, θ is the complement of the incidence angle, and ct is the time coordinate in displacement units (c is the velocity of light). These coordinates are indicated in Figure 2. There is no variation in the x coordinate which is out of the paper. The retarded time is zero when the gamma front passes a point, and τ can be regarded either as the distance of a point behind the gamma front, or as the time after passage of the gamma front. In our discussions we will take the former point of view and think of τ as a space variable.

Changing to the variables (τ,η) yields a set of first order partial differential equations. These equations have been differenced and

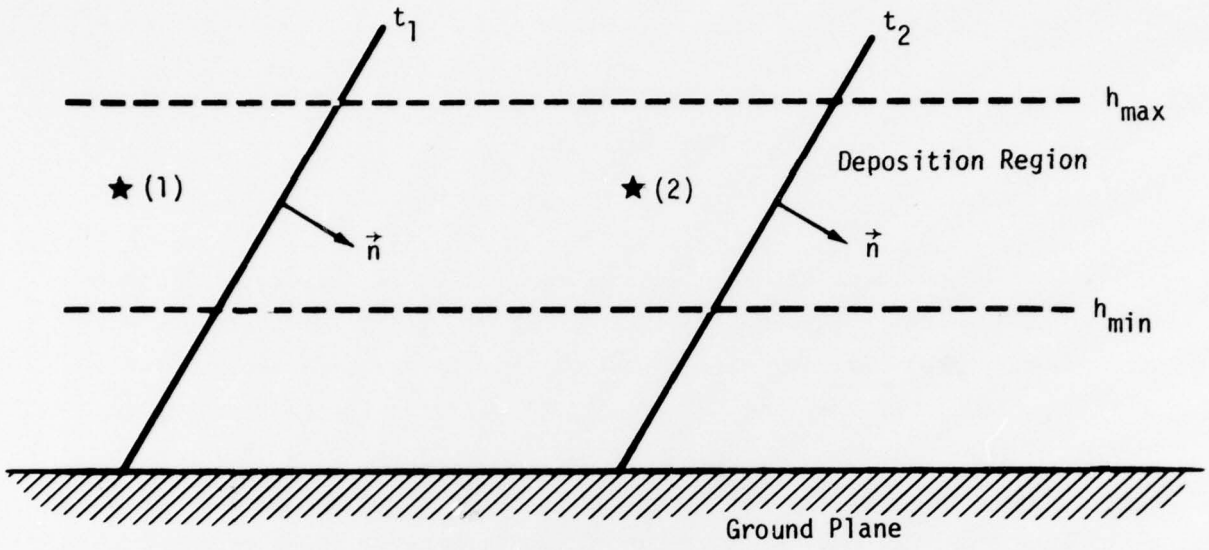

Figure 1. Far-plane approximation of LHAP.

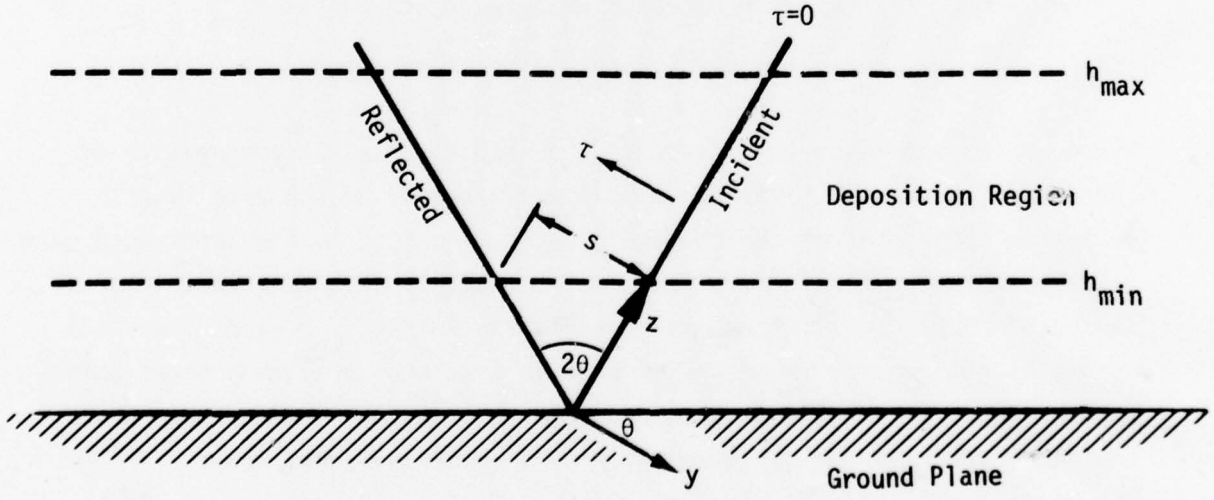

Figure 2. Incident and reflected wave fronts.

using LHAP we can calculate their solutions by integrating forward in the variable τ. Near the gamma-ray front this gives the correct solution. As indicated in Figure 2, further to the left of the incident wave there will be a region affected by EM fields reflected from the earth. These reflected waves will begin to have influence at the point where $\tau = s$, where s is the distance between incident and reflected wave fronts at the bottom of the deposition region. This distance is given by the following formula,

$$s = 2(\sin\theta)h_{min} \quad , \tag{2}$$

where h_{min} is the nominal altitude of the bottom of the deposition region. Before relating how these waves are incorporated into LHAP, we will describe how the reflected amplitudes may be calculated.

SECTION 3
THE REFLECTED WAVE

During the interval $0<\tau<s$ we have a complete solution for the fields at mesh points throughout the deposition region. As one approaches the lower boundary of this region along a wave front (τ constant), the currents and conductivity become negligible and the fields approach constant values. The wave form along the bottom of the deposition region is assumed to be that which reaches the earth.

We need to calculate the reflection of this wave. Scott[6] has made measurements of the dielectric constant and conductivity of many soil samples, and has found that they are functions chiefly of the water content of the soil and of the frequency of a monochromatic wave. An RC network model, in which the resistances depend on water content, was fitted to Scott's data by Longmire and Smith.[7] Using this information and the Fresnel formulae for reflection coefficients,[3] it is a straightforward matter to calculate the reflected wave form.

A convenient way to calculate the reflected wave form is by use of the impulse response. Let the incident electric field be the impulse function $\delta(t)$. The Fourier transform of this function is unity. Multiplying by the Fresnel reflection factor $\rho(\omega)$ (a complex function), we see that the impulse response is $\rho(\omega)$ in the frequency domain. In the time domain, the impulse response is the Fourier inverse,

$$G(t) = \frac{1}{2\pi}\int_{-\infty}^{\infty}\rho(\omega)e^{-i\omega t}\,dt \quad . \tag{3}$$

If the reflection factor is approximated as a sum of simple poles,

$$\rho(\omega) = \rho_\infty + \sum_{n=1}^{N} \frac{a_n}{b_n - i\omega} \quad , \tag{4}$$

where ρ_∞ is the infinite frequency reflection coefficient and a_n, b_n are a set of expansion parameters, the impulse response becomes

$$G(t) = \rho_\infty \, \delta(t) + \theta(t) \sum_{n=1}^{N} a_n \, e^{-b_n t} \quad . \tag{5}$$

where $\theta(t) = 0$ for $t<0$ and $\theta(t) = 1$ otherwise.

If we now have an incident field $E_i(t)$, the reflected field is the convolution

$$E_r(t) = \int_{-\infty}^{t} E_i(t')G(t-t')dt' \tag{6}$$

$$= \rho_\infty E_i(t) + \sum_{n=1}^{N} a_n \, Q_n(t) \quad . \tag{6'}$$

where we define

$$Q_n(t) = \int_{-\infty}^{t} E_i(t') \, e^{-b_n(t-t')} \, dt' \quad . \tag{7}$$

We see that Q_n satisfies the simple differential equation

$$\frac{dQ_n}{dt} = E_i(t) - b_n Q_n \quad . \tag{8}$$

Since the finite difference code LHAP advances the incident field one step at a time, it is a simple matter to advance the Q_n at each time step by use of Equation 8, and then to obtain $E_r(t)$ from Equation 6'. This is much easier than doing the convolution Equation 6 at each time.

The incident wave at the ground actually has two components of electric field, one in the plane of incidence (E_z) and one perpendicular to it (E_x). The two components have different reflection factors, each of which have to be fitted by the form Equation 4. The time delay for the wave to travel from the bottom of the deposition region to the ground and back must be taken into account.

The method used here of converting a convolution integral into a set of differential equations has been used previously by Longmire and Koppel.[6]

The method for determining the expansion parameters ρ_∞, a_n, b_n is described in the Appendix.

Figure 3 shows a typical incident electromagnetic wave from LHAP (up to 10^{-4} second) and its reflection from the earth. The reflection is shown without time delay, i.e., for an observer just above the ground. For this example we assumed a soil with ten percent water content and an incidence angle of 30°. For the LHAP application, we need to carry the reflection to later times, of course.

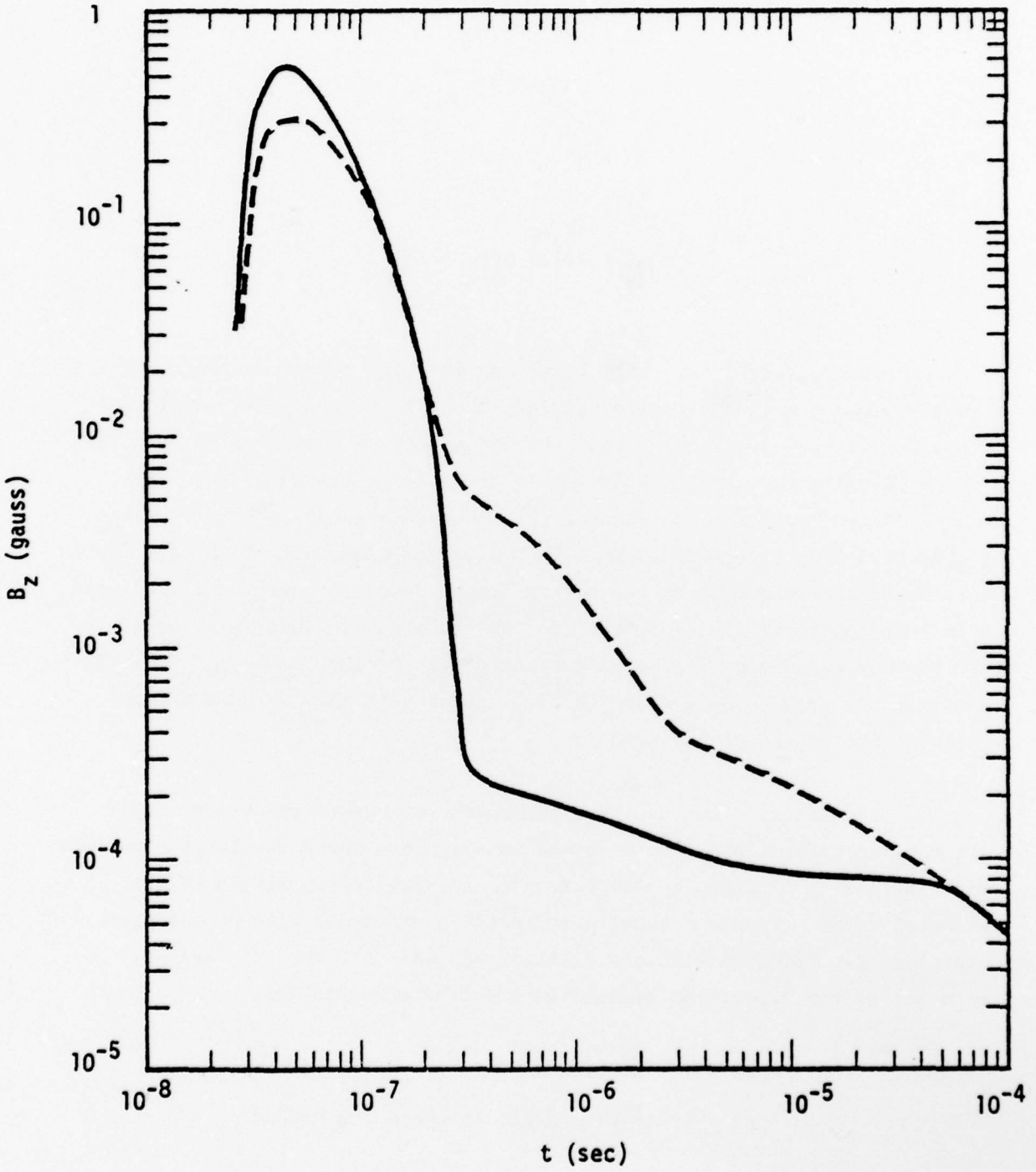

Figure 3. Typical wave forms from LHAP. Solid curve is incident wave and dashed curve is reflected wave.

SECTION 4
MODIFICATION OF LHAP

The reflected wave will travel up into the deposition region where it will interact with the ionized medium that lingers there. A portion of this wave will be reflected by the ionized medium and converted again into a downward-going wave, which will add to the wave generated by the late Compton current sources. The sum of these downward-going waves will again be reflected from the ground, etc. LHAP will calculate all of these effects if its boundary condition at the bottom of the deposition region is modified to include the total fields reflected from the ground. That is, we must take the downward-going fields at the bottom of the LHAP mesh (h_{min}), reflect them from the ground, delay them in time, and insert them as upward-going fields at the bottom of the mesh.

From Figure 3 we see that the earth-reflected wave varies rapidly with time at early times. In order to handle these short wavelengths without requiring a fine η mesh, we shift to a coordinate system fitted to the reflected waves. Figure 4 shows a reflected gamma front with propagation direction $\vec{n}'$ and Cartesian coordinates y' and z'; the x' axis is again out of the paper. We define the independent variables

$$\begin{aligned} \tau' &= ct - y' = \text{retarded time for reflected wave} \\ \eta' &= z' + (\tan\theta)y' = \text{slant height above ground} \end{aligned} \tag{9}$$

Note that τ' is zero on the reflected gamma front, so that there will be no reflected fields for $\tau'<0$. The high frequency reflected fields arrive just after $\tau' = 0$, so that a fine τ' mesh will be required here. Later

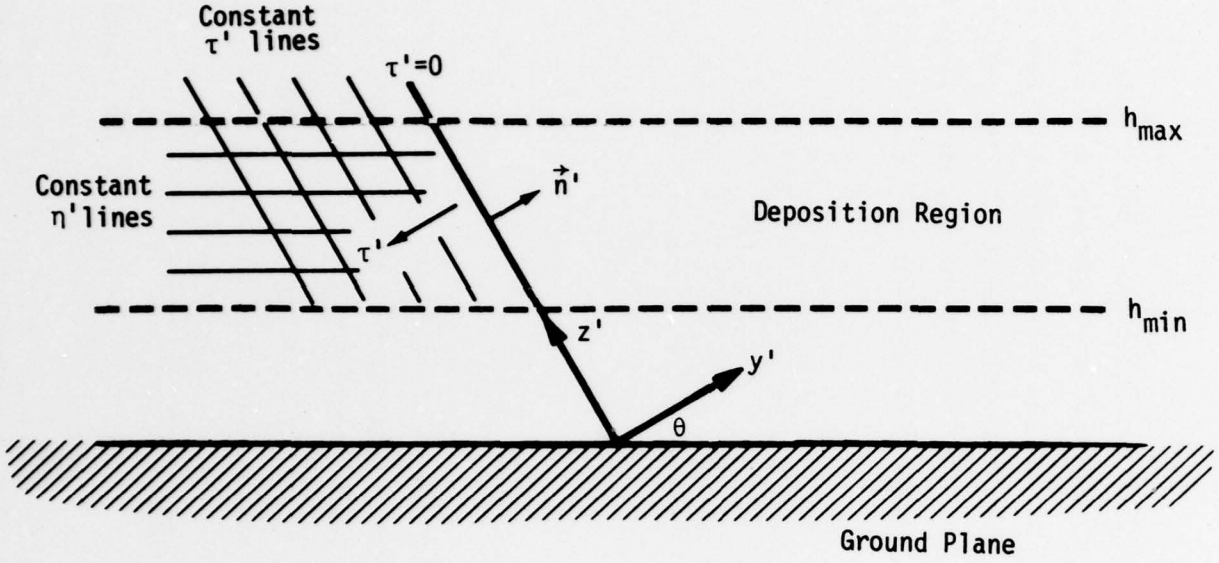

Figure 4. The reflected frame.

the τ' mesh can be expanded, since the reflected fields change more slowly. A fine η' mesh is not required. This is the reason for using the retarded time; all of the rapid variations are put into this variable and removed from the other.

Equations 9 differ from Equations 1 only in the sign of the $\tan\theta$ term. In the earlier LHAP writeup[2] a parameter b is defined as $\tan\theta$. The form of Maxwell's equations and the field variables of that report for the incident wave frame can be immediately adapted for the reflected frame by replacing b by -b. Thus, in terms of the Cartesian field components along the x', y' and z' axes, the modified LHAP will use the field variables $E_{y'}$, $B_{y'}$, and

$$\begin{aligned} H_{x'} &= E_{x'} + B_{z'} + bB_{y'} \\ Q_{x'} &= E_{x'} - B_{z'} + \frac{1}{b} B_{y'} \\ H_{z'} &= E_{z'} - B_{x'} + bE_{y'} \\ Q_{z'} &= E_{z'} + B_{x'} - \frac{1}{b} E_{y'} \end{aligned} \tag{10}$$

These equations replace Equations 1-14 of Reference 2. The inverse of the relations (10) and Maxwell's equations for all of the field quantities are given by Equations 1-15 and 1-16 of Reference 2, with b replaced by -b. We shall not rewrite these equations here, but note some useful properties. First, it is clear that the new Cartesian field components are related to the old ones by a rotation through angle 2θ about the x (or x') axis. Thus, for the electric field components,

$$\begin{aligned} E_{x'} &= E_x \\ E_{y'} &= (\cos 2\theta)E_y + (\sin 2\theta)E_z \\ E_{z'} &= -(\sin 2\theta)E_y + (\cos 2\theta)E_z \end{aligned} \tag{11}$$

and similar relations hold for the magnetic field components. For the H's and Q's, one can then show, with the help of some trigonometry, that

$$
\begin{aligned}
H_{x'} &= H_x \quad (=0 \text{ everywhere}) \\
Q_{x'} &= 2E_x - Q_x = H_x + \frac{2}{\sin 2\theta} B_y \\
H_{z'} &= H_z \quad (=0 \text{ below source region}) \\
Q_{z'} &= 2B_x - Q_z = - H_z - \frac{2}{\sin 2\theta} E_y
\end{aligned}
\tag{12}
$$

Again the Q's represent transverse waves and the H's longitudinal waves.

In the regions outside the source region, both of the longitudinal waves vanish, and the fields are the superposition of transverse waves propagating downward (in the direction $\vec{n}$) and upward (in the direction $\vec{n}'$). For each of the four transverse waves (two down, two up), the electric and magnetic fields are equal but perpendicular to each other. We shall specify the amplitudes of these four waves by giving the x (or x') component of the electric or magnetic field in the down (d) or up (u) cases. In terms of the LHAP field variables these amplitudes are:

$$
\begin{aligned}
E_{xd} &= \frac{1}{2} Q_x = - B_{y'}/\sin 2\theta \\
B_{xd} &= \frac{1}{2} Q_z = E_{y'}/\sin 2\theta \\
E_{xu} &= \frac{1}{2} Q_{x'} = B_y/\sin 2\theta \\
B_{xu} &= \frac{1}{2} Q_{z'} = - E_y/\sin 2\theta
\end{aligned}
\tag{13}
$$

These amplitudes will be used in applying the boundary conditions at the top and bottom of the source region.

In Figure 2, the fields in the region between the incident front and the reflected front are to be calculated by the previous version of LHAP. On the reflected front $\tau' = 0$, the coordinate system and the field variables are changed to the new system, which is retained for the duration of the LHAP calculation. Fields on the reflected front are put in as initial values for the fields in τ', using Equations 11 and 12.

We now discuss the boundary conditions to be applied at the top (h_{max}) and the bottom (h_{min}) of the η' mesh. At the top, the reasonable boundary condition is that there are no downward-going waves. This condition is met by setting $B_{y'} = E_{y'} = 0$ at that boundary, according to the first two of Equations 13. This parallels the procedure used in the original LHAP, where $B_y = E_y = 0$ at the bottom of the mesh to impose the boundary condition of no upward-going waves.

At the bottom of the η' mesh (h_{min}), we pick out the amplitudes E_{xd} and B_{xd} of the downward-going waves, using the first two of Equations 13. Each of these amplitudes is reflected from the ground, using the procedure developed in Section 3. The reflected amplitudes, when properly delayed in time to

$$\tau'_{ref} = \tau'_{inc} + 2(\sin\theta)h_{min} \quad , \tag{14}$$

give the values of E_{xu} and B_{xu}. These values determine boundary values for $Q_{x'}$ and $Q_{z'}$ from the last two of Equations 13.

These boundary values, including $B_{y'} = E_{y'} = 0$ at the top, are sufficient to determine the solution in the source region. The two-sweep algorithm used in LHAP is again applicable. Two trial values for $B_{y'}$ and $E_{y'}$ at the bottom are assumed and the equations integrated upward in η' until the top is reached, thus obtaining two trial solutions. The true solution is then the linear combination of these which satisfies the boundary conditions at the top.

SECTION 5
SUMMARY

A fast method has been developed for computing the EMP waves reflected from the ground. The LHAP code has been modified to accept the reflected waves, which is necessary if LHAP is to compute beyond retarded times of about 100 microseconds. A short test problem was run, and the code appears to be working properly. Longer problems will be run in the coming year, when we apply it to problems of interest in EMP environments. We expect to calculate to times of the order of one millisecond, by which time the prompt-gamma-driven EMP should be finished.

REFERENCES

1. Longmire, C. L., private communication.

2. Longley, H. J., R. M. Hamilton, and C. L. Longmire, private communication.

3. Stratton, J. A., Electromagnetic Theory, McGraw-Hill, New York (1941).

4. Messier, M. A., The Effect of Ground Reflection on Observed EMP Waveforms, MRC-R-78, DNA 3370T, Mission Research Corporation, September 1974.

5. Marx, E., "Reflected and Transmitted Fields for a Plane-Wave Pulse Incident on a Conducting Ground," Harry Diamond Laboratory, TR-1740, April 1976.

6. Scott, J. H., "Electrical and Magnetic Properties of Rock and Soil," United States Geological Survey Technical Letter, Special Project-16, May 1966; also appears as Note VIII in DASA 1882-1, "Electromagnetic Pulse Theoretical Notes, Vol. I, May 1967.

7. Longmire, C. L., and K. Smith, A Universal Impedance for Soils, MRC-N-214, DNA 3788T, Mission Research Corporation, October 1975.

8. Longmire, C. L., and J. Koppel, "Formative Time Lag of Secondary Ionization," Mission Research Corporation, MRC-R-88, January 1974.

APPENDIX
FITTING OF THE IMPULSE RESPONSE

We desire to fit the impulse response function $G(t)$ as a sum of decaying exponentials. As discussed in the text one method of doing this involves the inverse Fourier transform of the reflection coefficients. A simpler procedure utilizes the Laplace transform since the analysis will then involve only real variables.

It is useful to conceptualize the problem as an exponentially rising test wave incident on the ground,

$$E_i = E_o \exp(st) \quad . \tag{A1}$$

The reflection of this wave will also be an exponentially rising wave with the same rate,

$$E_r = \rho E_o \exp(st) \quad . \tag{A2}$$

The reflection coefficient for this wave has the same form as that for a traditional Fourier wave with s substituted for $i\omega$. For the case with the electric field vector E perpendicular to the plane of incidence, the reflection coefficient is given by

$$\rho_\perp = \frac{s\cos\theta - \sqrt{s(\varepsilon s+4\pi\sigma c) - s^2\sin^2\theta}}{s\cos\theta + \sqrt{s(\varepsilon s+4\pi\sigma c) - s^2\sin^2\theta}} \tag{A3}$$

When E is parallel to the plane of incidence,

$$\rho_{\parallel} = \frac{(\varepsilon s+4\pi\sigma c)\cos\theta - \sqrt{s(\varepsilon s+4\pi\sigma c) - s^2\sin^2\theta}}{(\varepsilon s+4\pi\sigma c)\cos\theta + \sqrt{s(\varepsilon s+4\pi\sigma c) - s^2\sin^2\theta}} \qquad \text{(A4)}$$

In these, θ is the incidence angle, ε and σ are the dielectric coefficient and conductivity of the earth respectively, and c is the speed of light. Note that these are both pure real expressions. The term $(\varepsilon s+4\pi\sigma c)$ is the admittance of the soil in cgs units. It is straightforward to evaluate this term when the earth is approximated as a RC network, as was done by Longmire and Smith.[7]

Instead of inverse Laplace transforming these reflection coefficients, we transform the response function and make the fit in the s-domain. The Laplace transform of Equation 5 is

$$\tilde{G}(s) = \rho_{\infty} + \sum_{n=1}^{N} \frac{a_n}{b_n+s} \qquad \text{(A5)}$$

We chose a ρ_{∞} and a set of a_n and b_n so that this function is a good approximation of the reflection coefficient. $\rho_{\perp}$ and $\rho_{\parallel}$ must be separately approximated.

The fitting procedure is as follows. Let t_{min} and t_{max} be the minimum and maximum times of interest. In the case of LHAP these are

$$t_{min} \approx 10^{-9} \text{ sec}$$
$$t_{max} \approx 10^{-3} \text{ sec} \quad . \qquad \text{(A6)}$$

Then, from the Fresnel reflection factors for the soil and angle of interest, calculate $\rho(s)$ over the range $s_{min} \leq s \leq s_{max}$, where

$$s_{min} = 1/t_{max} \approx 10^3$$

$$s_{max} = 1/t_{min} \approx 10^9 \quad . \tag{A7}$$

$\rho(s)$ will be a decreasing function of s, but will not fall as fast as $1/s$. Now choose a set of frequencies b_n to cover the range of s. Our experience indicates that one frequency per decade will yield an adequately accurate approximation. Next, determine the ρ_∞ and set of a_n's such as to give the least-squares best fit to $\rho(s)$ using Equation A5 at several values of s; say, $s = 10^3$, 3×10^3, 10^4, ..., 10^9. Finally, calculate the fit at many values of s and compare with $\rho(s)$. Better fits will be obtained by using more terms b_n and a_n.

In the following table and figure we present results of a fit to our example problem with a 30° incidence angle and a soil with a 10 percent water content. Because of the conductivity, $\rho(s)$ goes to unity for $s = 0$. Although we do not need to fit for $s \lesssim 10^3$ for the LHAP application, we note that our procedure gives

$$\tilde{G}(o) = \rho_\infty + \sum_{n=1}^{N} \frac{a_n}{b_n} = 0.99968 \quad , \tag{A8}$$

which is in excellent agreement. At the opposite extreme, the infinite frequency reflection coefficient involves only the dielectric properties of the soil. Assuming the infinite frequency relative dielectric coefficient to be 5 (see Reference 7), ρ_∞ has an analytic value of 0.432, somewhat below our fit value. Our procedure has lumped the responses faster than 10^{-9} sec with the delta function. In the figure we also show the response function with 25 exponentials as the dashed line. The close agreement of these curves makes it clear that we have obtained an excellent fit.

Table 1. Expansion parameters for the reflection coefficient of wave with E-field perpendicular to plane of incidence. The soil has a water content of ten percent, and the incidence angle is 30°.

i	$a_i(sec^{-1})$	$b_i(sec^{-1})$	a_i/b_i
1	2.0257	10^3	0.00203
2	2.8295×10	10^4	0.00283
3	1.5070×10^3	10^5	0.01507
4	3.5470×10^4	10^6	0.03547
5	1.3212×10^6	10^7	0.13212
6	1.7462×10^7	10^8	0.17462
7	1.0890×10^8	10^9	0.10890
Delta Function Coefficient		ρ_∞	0.52864
		Sum:	0.99968

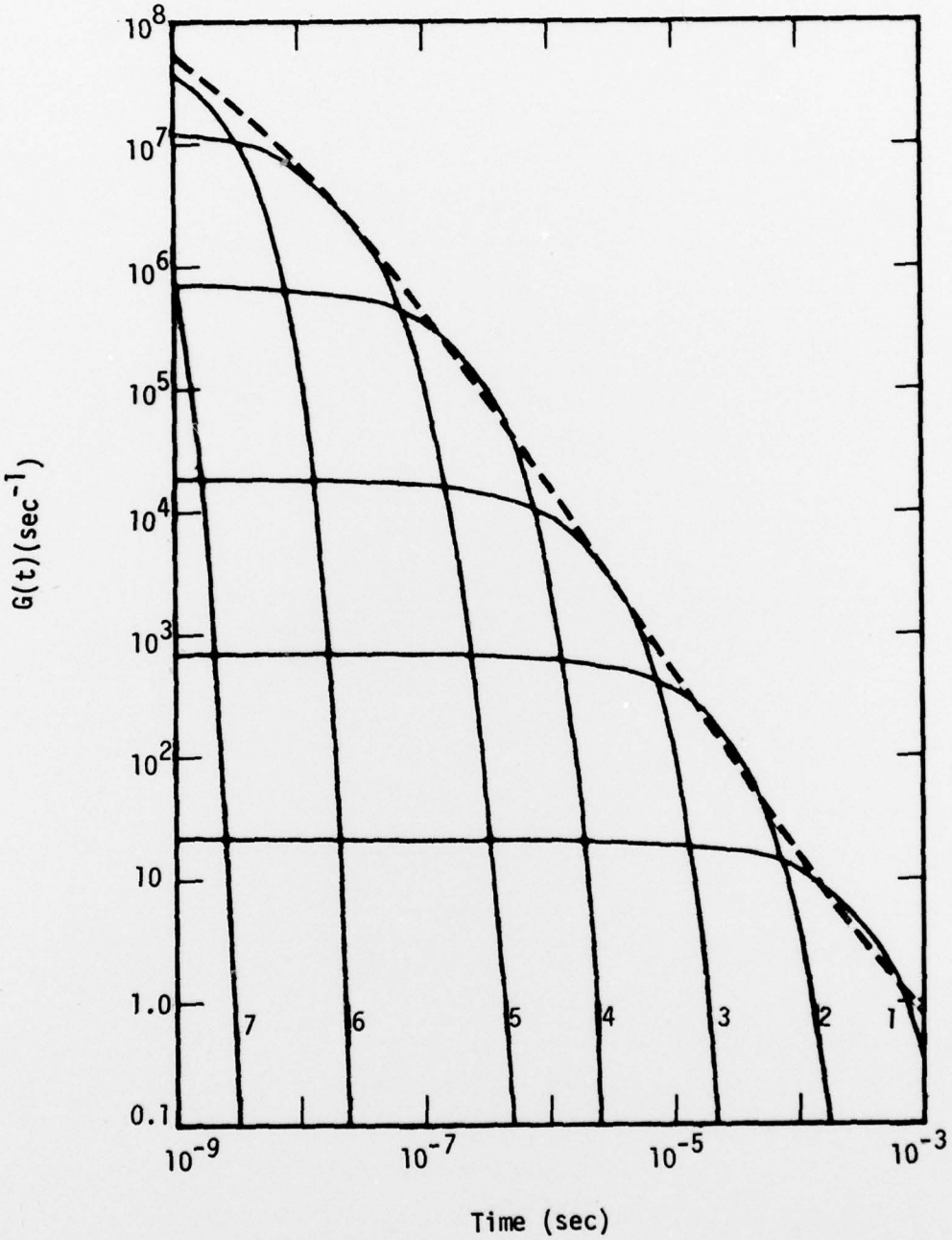

Figure 5. Response function. The solid lines are the exponentials of Table 1. The dashed line is the response function using 25 exponentials.

DISTRIBUTION LIST

DEPARTMENT OF DEFENSE

Assistant to the Secretary of Defense
Atomic Energy
ATTN: Executive Assistant

Defense Civil Preparedness Agency
Assistant Director for Research
ATTN: TS AED

Defense Communication Engineer Center
ATTN: Code R720, C. Stansberry

Defense Communications Agency
ATTN: CCTC C313
ATTN: CCTC C312

Defense Documentation Center
Cameron Station
12 cy ATTN: TC

Defense Nuclear Agency
ATTN: DDST
4 cy ATTN: TITL

Interservice Nuclear Weapons School
ATTN: Document Control

Joint Strat. Tgt. Planning Staff
ATTN: JSAS
ATTN: JPST

Livermore Division, Fld. Command, DNA
Lawrence Livermore Laboratory
ATTN: FCPRL

Under Secy. of Def. for Rsch. & Engrg.
ATTN: Strategic & Space Systems (OS)

DEPARTMENT OF THE ARMY

ERADCOM Technical Support Activity
ATTN: E. Hunter
ATTN: DRSEL-TL-ME
ATTN: DRSEL-TL-MD, G. Gaule

Harry Diamond Laboratories
ATTN: DELHD-RBA
ATTN: DELHD-EM
ATTN: W. Wyatt
ATTN: DELHD-NP
2 cy ATTN: DELHD-RBC

U.S. Army Electronics Rsch. & Dev. Command
ATTN: DRCPM-ATC

U.S. Army Intelligence & Sec. Cmd.
ATTN: Technical Information Facility

DEPARTMENT OF THE NAVY

Naval Ocean Systems Center
ATTN: Code 015, C. Fletcher

DEPARTMENT OF THE NAVY (Continued)

Naval Research Laboratory
ATTN: Code 6623, R. Statler
ATTN: Code 4104, E. Brancato

Naval Surface Weapons Center
Dahlgren Laboratory
ATTN: Code DF-56

DEPARTMENT OF THE AIR FORCE

Air Force Technical Applications Center
ATTN: TFS, M. Schneider

Air Force Weapons Laboratory, AFSC
ATTN: NXS
ATTN: ELP, W. Page
ATTN: NTN

Foreign Technology Division
Air Force Systems Command
ATTN: NICD, Library

DEPARTMENT OF ENERGY

Lawrence Livermore Laboratory
ATTN: Doc. Con. for L-156, E. Miller
ATTN: Doc. Con. for L-153, D. Meeker
ATTN: Doc. Con. for L-156, H. Cabayan

Los Alamos Scientific Laboratory
ATTN: Doc. Con. for B. Noel

Sandia Laboratories
ATTN: Doc. Con. for E. Hartman
ATTN: Doc. Con. for C. Vittitoe

DEPARTMENT OF DEFENSE CONTRACTORS

Boeing Co.
ATTN: H. Wicklein

Computer Sciences Corp.
ATTN: R. Dickhaut

Dikewood Industries, Inc.
ATTN: K. Lee

General Electric Co.
Aerospace Electronics Systems
ATTN: C. Hewison

General Electric Co.
ATTN: Technical Library

General Electric Co.-TEMPO
Alexandria Office
ATTN: DASIAC

General Research Corp.
Santa Barbara Division
3 cy ATTN: Technical Information Office

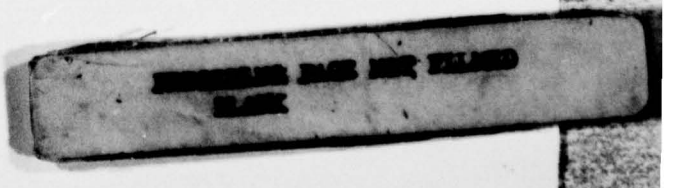

DEPARTMENT OF DEFENSE CONTRACTORS (Continued)

Georgia Institute of Technology
Office of Contract Administration
ATTN: Rsch. Security Coordinator for H. Denny

GTE Sylvania, Inc.
Electronics Systems Grp., Eastern Div.
ATTN: L. Blaisdell

IIT Research Institute
Electromag Compatability Anal. Ctr.
ATTN: ACOAT

Kaman Sciences Corp.
ATTN: J. Lubell
ATTN: W. Stark

Lockheed Missiles & Space Co., Inc.
ATTN: B. Kimura
ATTN: M. Bernstein

Mission Research Corp.
ATTN: W. Hobbs
2 cy ATTN: C. Longmire
5 cy ATTN: Document Control

DEPARTMENT OF DEFENSE CONTRACTORS (Continued)

R & D Associates
ATTN: M. Grover
ATTN: J. Bombardt
ATTN: C. MacDonald

Rand Corp.
ATTN: W. Sollfrey

Science Applications, Inc.
Huntsville Division
ATTN: N. Byrn

Systems, Science & Software, Inc.
ATTN: A. Wilson

TRW Defense & Space Sys. Group
ATTN: R. Plebuch
ATTN: H. Holloway
ATTN: W. Gargaro

Northrop Corp.
Electronic Division
ATTN: Radiation Effects Group